A Sublimation Model for the Martian Polar Swiss-Cheese Features

Shane Byrne[1] and Andrew P. Ingersoll[1]

Email: shane@gps.caltech.edu

[1] Division of Geological and Planetary Sciences, California Institute of Technology, Pasadena, California 91125.

Submitted to Science

Submitted 4th November 2002

In their pioneering work Leighton and Murray argued that the Mars atmosphere, which is 95 percent CO_2 today, is controlled by vapor equilibrium with a much larger polar reservoir of solid CO_2. Here we argue that the polar reservoir is small and cannot function as a long-term buffer to the more massive atmosphere. Our work is based on modeling the circular depressions (Swiss-cheese features) in the south polar cap. We argue that a solid CO_2 layer ~8 meters thick is being etched away to reveal water ice underneath. Preliminary results from the THEMIS instrument seem to confirm our model.

In 1966 Leighton and Murray (1) proposed that the polar caps constitute a permanent reservoir of CO_2, much larger than the atmospheric reservoir, whose vapor pressure determines the average surface pressure on Mars. The north pole was the favored location (2) because its lower elevation allows the CO_2 ice to equilibrate with the atmosphere at a higher temperature and pressure than in the south. Viking observations showed just the opposite—that the north pole loses its seasonal covering of CO_2 each year although the south cap does not (3). The north residual cap—the part that survives the summer—is therefore water ice (4), which is much less volatile than CO_2. The survival of solid CO_2 in the south might be due to its cleanliness (lack of dust) and consequent high albedo, which allows it to absorb less sunlight (5).

In 1969 there was an unusual amount of water vapor over the south pole in summer (6), suggesting that the covering of solid CO_2 had partially disappeared and had exposed water ice underneath. The implication is that the covering is only a few meters thick (7) and could not function as a buffer for the atmosphere on time scales over which orbital elements are changing. A further complication is that solid CO_2 does not possess sufficient strength (8, 9) to support the 3-kilometer topographic bulge that is observed at both poles by MOLA (9). The implication is that both polar caps are largely water ice although a thin veneer of CO_2 covers the south cap. The thickness of this residual CO_2 layer bears directly on the question of the global inventory of this important volatile.

Figure 1 shows a high resolution MOC image (10) of the southern residual polar cap at L_s 211° (L_s is an angular measure of Mars' position in its orbit, with southern spring

spanning L_s 180° to L_s 270°). The quasi-circular depressions with flat floors and steep sided walls are the so-called Swiss-cheese features (11). Although they range in lateral size from a few hundred meters to a kilometer or two, the depth inferred from shadow measurements is ~8 m (11). In a few cases we confirmed this depth directly by comparing MOC images with MOLA altimetry. The larger depressions commonly display an interior moat running around the inside of their walls. In some of the highest-resolution MOC frames the walls appear layered, with individual light and dark bands each 1-2 meters thick (11). Although the depressions are generally circular, they do exhibit a slight asymmetry in the form of a small cusp that points toward the south pole.

Figure 2 shows a portion of the residual cap in spring and summer, L_s 246° and L_s 327°, respectively. In summer the walls of the depressions are much darker (12) than the flat floors and the surrounding flat upper surfaces (the mesa tops). The walls also expand outward at rates of 1-3 meters per year (13). Their diameters are growing at twice this rate. This rate of retreat is only possible if the medium in which the depressions are imbedded is volatile, *i.e.*, it must be CO_2. All depressions in any one area are roughly the same size (Fig. 1), indicating that the differences in the time they all formed is small compared to their growth time.

We have created a model (14) to investigate the growth of circularly symmetric depressions of arbitrary cross section. The shape of the depression evolves as a function of time as CO_2 condenses and sublimes in response to solar and infrared radiation. In assuming circular symmetry, we are neglecting the slight difference in diurnally averaged

insolation (incident sunlight projected onto the surface) between the north and south sides of the depressions, provided they are within a few degrees of the pole. The model (14) accounts for incident short-wave radiation (including shadowing), emitted thermal radiation, and all orders of scattered long and short wave radiation.

Although we experimented with many model parameters, only two cases give flat floors, steep sides, and rapidly retreating walls. In both cases an active slab ~8 m thick overlies a less active substrate. The active slab is dirty (low-albedo) CO_2 frost, although we assign higher albedos to new CO_2 frost that formed over the previous winter. The less active substrate may be either water ice or clean (high-albedo) CO_2. The albedo of the clean CO_2 is the same as that of the mesa tops and is adjusted so that these surfaces neither gain nor lose net mass over the course of a year. The CO_2 temperature is fixed year-round by contact with the atmosphere. The water ice may warm up when it is exposed in the summer. This heat is conducted downward and is available to partially offset the condensation of CO_2 the next winter. Sublimation of water ice is assumed to be negligible.

Figure 3A shows model output when the albedo and emissivity are the same for the walls and the surrounding flat mesa top. The initial size and shape of the depression do not affect the subsequent behavior. In all these cases the depressions disappear into the surrounding terrain, *i.e.*, their depth to diameter ratio shrinks. This is due both to infilling of the depression floor and lateral expansion of the depression walls. We find the same

infilling (not shown) when the albedo increases with insolation as suggested by Viking observations (5).

Figure 3B shows what happens when the flat surfaces and seasonal CO_2 frost have a high albedo (~0.7) and the residual frost has a low albedo (~0.5). The depression expands but it maintains its bowl shape and does not develop a flat floor, which is an important characteristic of the observed Swiss-cheese depressions.

Figure 4A shows a case with a water ice substrate. Above the substrate there is a low-albedo slab whose thickness we varied from 4 to 20 meters and whose albedo we varied from 0.40 to 0.65. Once the bright seasonal frost has been removed, the darker-albedo CO_2 frost is exposed to insolation, causing this initial indentation to grow downward in a way similar to that in Fig. 3B. This growth proceeds until the depression encounters the water ice, after which the floor remains flat from one year to the next and the walls move outward. The slopes of the walls eventually steepen to about 10°, which is less than the typical observed slopes (20° to 40°), although in some cases (Fig. 2C of Ref. 11) the slopes are smaller.

In Fig. 4B we allow the albedo of the dirty CO_2 slab to decrease with depth. This case is pictured in Fig. 5B. The lower albedo at the bottom of the slab causes the walls to steepen. The water ice below the slab insures that the floor remains flat. The depression grows down to the substrate during the ramp-up phase, and then the walls recede outward during the linear growth phase. With a slab 4 m thick, the depressions reach the linear

growth phase within 30 Martian years. With a slab 20 m thick, the ramp-up phase lasts for 300 Martian years. The growth rate is larger when the albedo is lower. With an albedo of 0.4 at the base of the slab (Fig. 5B) the growth rate is ~2.5 m yr^{-1}. With an albedo of 0.65 at the base of the slab the growth rate is ~1.0 m yr^{-1}. These values span the uncertainties in the growth rates (13) and albedos measured in the MOC images.

Replacing the water ice substrate (Fig. 5B) with a clean CO_2 substrate (Fig. 5A) has almost no effect. The evolution of the depressions again follows that illustrated in Fig. 4. As in the water ice case, the evolution proceeds through a ramp-up phase to a linear growth phase. The growth rates depend on the albedo of the overlying slab as before.

To distinguish between these two cases (Fig. 5A and 5B), one needs to observe the temperature of the floors of the depressions. Solid CO_2 will always remain at the frost point, since it is in contact with the atmosphere. At the pressures on top of the south polar cap, this temperature is ~142 K. Water ice is not subject to this constraint, and when it is exposed in late summer ($310° < L_s < 350°$), its temperature will rise. The maximum temperature occurs around L_s 320°. We estimate that an infrared instrument like TES (16) would see brightness temperatures of 145, 147, 149, and 152 K if the fraction of its field of view occupied by circular depressions were 10, 20, 30, and 40 percent, respectively. We looked for such signals in the TES data, but effects due to the variable opacity of the atmosphere led to an inconclusive result.

The THEMIS instrument on the Mars Odyssey spacecraft (16) has a spatial resolution of 100 m and therefore can resolve the larger depressions. Figure 6 shows a THEMIS image with a MOC image of the same area. The blue (cold) area at the bottom is the edge of the residual CO_2 cap. The red area is too warm to be CO_2. The MOC image shows that the cold arc in the middle of the warm area is an extended mesa top, with the characteristic scalloped sides where the circular depressions have eaten into the walls (Fig. 2). In this place, at least, one has a set of circular depressions whose floors cannot be CO_2 and whose mesa tops almost certainly are CO_2. This observation favors the case shown in Fig. 5B, in which a substrate of water ice underlies a thin slab of CO_2.

If the CO_2 residual cap is only ~10 meters thick in all areas, its importance as a permanent reservoir is small. With an area of 88,000 km^2, thickness of 10 m, and density of 1.6 g cm^{-3}, the cap would contribute only 0.36 millibar of additional atmospheric pressure if completely sublimed. This is roughly 5% of the average surface pressure, so unless there is an additional subsurface reservoir, the atmospheric pressure cannot increase above its current value regardless of other changes in the climate or orbital forcing. If the Martian CO_2 is mostly in the atmosphere, then the ratio of its mass to the planet's mass is much less than the corresponding ratios for the Earth and Venus.

Further analysis of THEMIS data would be useful (17). Further modeling would address issues of how the circular depressions are formed and how they interact with each other and with the mesa tops on a long time scale. The mass budget of the south polar cap is an open issue. It is possible that the flat surfaces (mesa tops and floors of the depressions)

are participating in a long-term redistribution of CO_2 ice from within the depressions to other parts of the residual cap. The role of dust is also open. We do not know how the upper CO_2 slab got its layers or why the walls are dirtier than freshly deposited CO_2. Presumably the dust is released as the CO_2 sublimes from the walls, but then it must get blown away since the floors are not as dark as the walls. The moats, the cusps, and the uniform size of the depressions within each larger area are not well understood. The last may be evidence of sudden climatic events that created the depressions within a given area all at the same time.

References and Notes

1. R.B. Leighton, B. C. Murray, *Science* **153**, 136 (1966).
2. B.C. Murray, M. C. Malin, *Science* **182**, 437 (1973).
3. H.H. Kieffer, *J. Geophys. Res.* **84**, 8263 (1979). H.H. Kieffer *et al.*, *Science* **194**, 1341 (1976).
4. C.B. Farmer *et al.*, *Science* **194**, 1339 (1976).
5. P.B. James, H.H. Kieffer, D.A. Paige., In *Mars,* H.H. Kieffer, B.M. Jakosky, C.W. Snyder, M.S. Mathews, Eds. (Univ. of Arizona Press, Tucson, AZ, 1992), pp 934-968. B.M. Jakosky, R.M. Haberle, *ibid*, pp 969-1016.
6. E.S. Barker *et al.*, *Science* **170**, 1308 (1970).
7. B.M. Jakosky, R. M. Haberle, *J. Geophys. Res.* **95**, 1359 (1990).
8. J.F. Nye *et al.*, *Icarus* **144**, 449 (2000). W.B. Durham *et al.*, *Geophys. Res. Lett.* **26**, 3493 (1999). P.M. Schenk, J. M. Moore, *J. Geophys. Res.* **105**, 24,529 (2000).
9. Smith *et al., Science* **284**, 1495 (1999).

10. M.C. Malin *et al.*, *J. Geophys. Res.*, **97**, 7699, (1992).

11. P.C. Thomas *et al.*, *Nature* **404**, 161 (2000).

12. M.C. Malin, K. S. Edgett 2001, *J. Geophys. Res.* **106**, 23429 (2001).

13. M.C. Malin, *et al.*, *Science* **294**, 2146 (2001).

14. We use a matrix inversion approach ("radiosity") as described by Vasavada *et al.*, *Icarus* **141**, 179 (1999) to calculate all orders of scattering. By assuming circular symmetry we only have to keep track of annular bands. All surfaces are assumed to be Lambert scatterers. The time step is 1° of L_s, which is ~2 days. We verified the model against the analytic solution for spherical bowl-shaped craters as described by Ingersoll *et al.*, *Icarus* **100**, 40 (1992).

15. P.R. Christensen *et al.*, *J. Geophys. Res.*, **97**, 7719, (1992).

16. P.R. Christensen *et al.*, *Space Science Reviews*, submitted (2002).

17. H.H. Kieffer, T.N. Titus, *Science*, submitted (2002).

18. We thank Oded Aharonson, Arden Albee, Bruce Murray, and Norbert Schorghofer for helpful comments and discussions. We also thank NASA's Mars Data Analysis Program and Mars Global Surveyor Project for financial support.

FIGURE CAPTIONS

Fig. 1. Sub-frame of MOC narrow angle image M07/04167, taken at 86.8° S, 5° W, L_s 211°, showing many Swiss cheese features. Arrows in this and other figures point to north (N) and to the Sun (*).

Fig. 2. Albedo changes when the seasonal CO_2 cover is removed and the residual CO_2 cap is exposed. Area is at 86° S, 349° W, sub-frames of M09/04708 and M13/02177 at L_s of 246° and 327° respectively.

Fig. 3. Model results for CO_2 only cases. The top panel (A) describes results for CO_2 with a constant albedo of 0.7, plotted every Martian century. The initial depression becomes shallower and will eventually disappear. The bottom panel (B) describes results with a darker residual frost (0.6 in this case). The initial depression expands as a bowl shaped feature and does not resemble Swiss-cheese features. Note the differing horizontal scales for each plot.

Fig. 4. Model results for a dark residual CO_2 slab overlying a water ice base. In the top panel (A) the albedo of the residual CO_2 is constant with depth and equal to 0.6. Fresh CO_2 has an albedo of 0.7. The depression acquires a flat floor but its walls remain shallow (~3°). In the bottom panel (B) there is a gradient of albedo in the CO_2 slab from 0.7 at the top to 0.6 at the bottom. The walls develop the characteristic steepness (~30°)

of Swiss-cheese features and move outward at rates (~1.1 m/yr) consistent with observations.

Fig. 5. Illustration of albedo versus depth for two cases that successfully reproduce Swiss-cheese depressions. Panel A shows an example of cases with a dirty slab of CO_2, which is underlain by a bright CO_2 substrate. Panel B is the same but with a water ice substrate and no albedo discontinuity. Albedo decreases with depth in the dirty CO_2 slab in both cases.

Fig. 6. Example of Swiss-cheese observed by THEMIS (I00826006) at the cap edge near 84° S, 77° W, L_s 330°. Top panel shows temperatures derived from THEMIS radiance measurements in a 10x5 km area. Boxed area corresponds to sub-frame of MOC narrow angle image M03/04994, shown in the bottom panel. Cold material corresponds to the CO_2 mesa-tops, and warm material corresponds to terrain surrounding the mesas and making up the floors of the Swiss-cheese. This data rules out the clean CO_2 substrate alternative in this area.

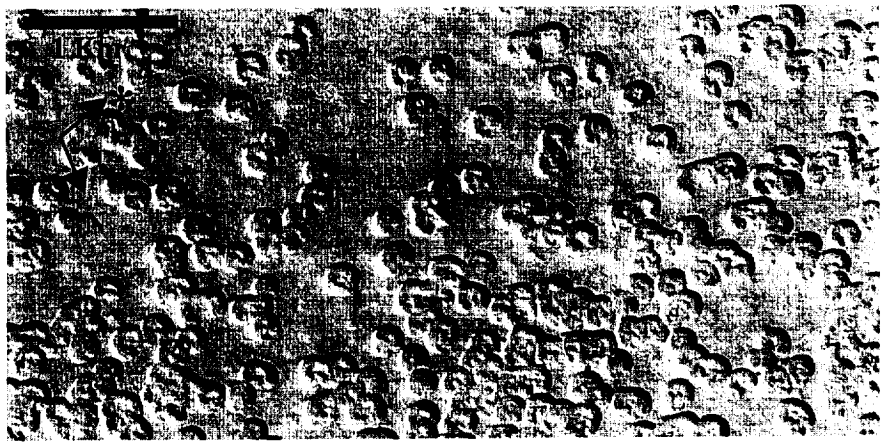

Figure 1: Byrne and Ingersoll

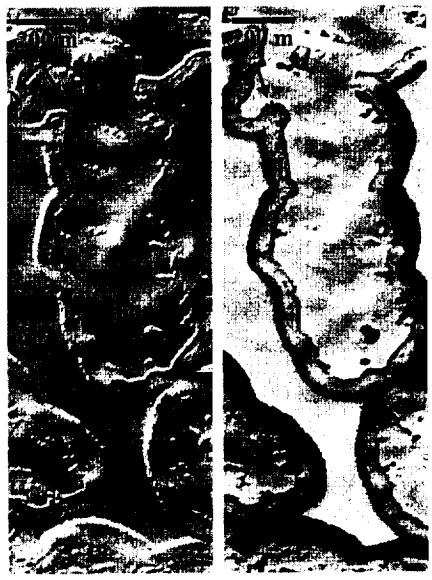

Figure 2: Byrne and Ingersoll

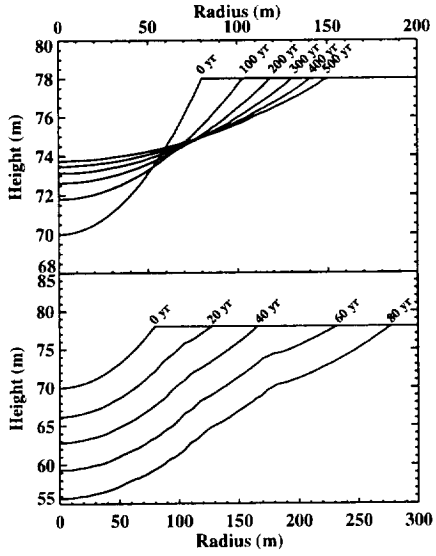

Figure 3: Byrne and Ingersoll

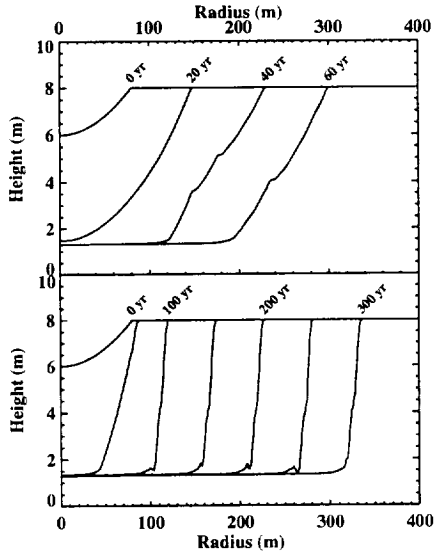

Figure 4: Byrne and Ingersoll

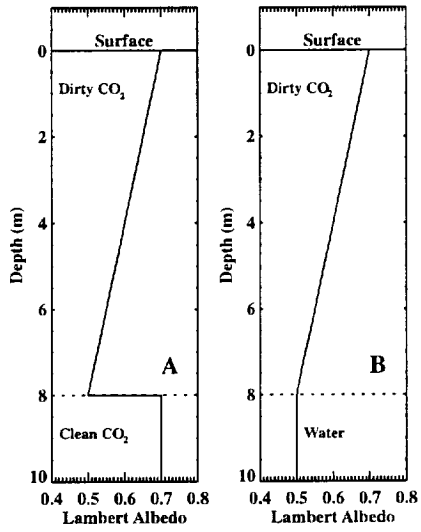

Figure 5: Byrne and Ingersoll

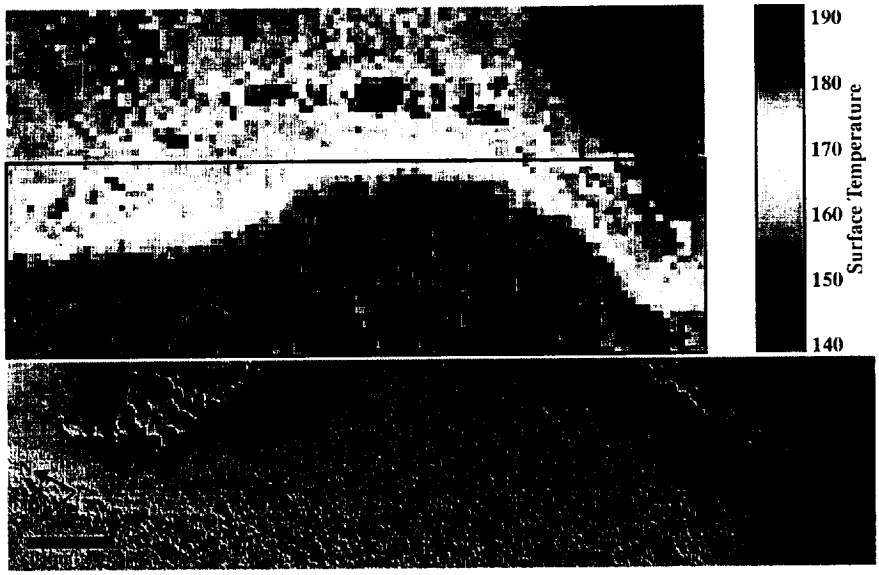

Figure 6: Byrne and Ingersoll